Laser and Particle Beams (2013), *31*, 531–537.
© Cambridge University Press, 2013 0263-0346/13 $20.00
doi:10.1017/S0263034613000311

Effect of plasma channel non-uniformity on resonant third harmonic generation

ANURAJ PANWAR,[1] CHANG-MO RYU,[1] AND ASHOK KUMAR[2]

[1]Department of Physics, POSTECH, Hyoja-Dong San 31, KyungBuk, Pohang, South Korea, 790-784
[2]Physics Department, ATAS, ASET, Amity University, Noida, Uttar Pradesh 201303, India

(Received 31 December 2012; Accepted 19 March 2013)

Abstract

We study the generation of resonant third harmonic laser radiation in a density non-uniform rippled plasma channel. An introduction of plasma channel non-uniformity strongly enhances the self-focusing and compression of main laser pulse at lower powers. In a deeper plasma channel, self-focusing is less sensitive to laser amplitude variation but increases compression. Plasma density ripple 'n_q' leading to resonant third harmonic generation when $k_q = 4\omega_p^2/3m_e\omega_0 c\gamma_0$, where '$\omega$'$_p$ is electron plasma frequency, 'ω_0' is laser frequency, and 'γ_0' is the electron Lorentz factor. Third harmonic is produced through the beating of ponderomotive force induced second harmonic density oscillations and the oscillatory velocity of electrons at main laser frequency. The self-focusing and compression of the fundamental pulse periodically enhances the intensity of the third-harmonic pulse at lower powers of main laser. In a deeper plasma channel, the third harmonic power is less effective by self-focusing and the compression of main laser, and increase with main laser pulse power.

Keywords: Plasma channel non-uniformity; Self-focusing; Third harmonic laser radiation

1. INTRODUCTION

Intense laser pulse propagation through plasma channels (Esarey *et al.*, 1997) has many application, including *x*-ray lasers (Korobkin *et al.*, 1996), high harmonic generation (Milchberg *et al.*, 1995) and laser-plasma accelerators (Esarey *et al.*, 2009). This has been experimentally demonstrated using plasma channels generated by hydrodynamic expansion (Durfee *et al.*, 1993; Durfee *et al.*, 1995; Nikitin *et al.*, 1997) or capillary discharges (Ehrlich *et al.*, 1996; Spence *et al.*, 2001) created the channel by a twin pulse scheme utilizing the cumulative effects of femtosecond pulse ignition and longer pulse assisted heating. Furthermore, plasma channels have been used to guide intense ($>10^{18}$ W/cm^2) laser pulses for laser-plasma accelerator experiments (Geddes *et al.,* 2004; Leemans *et al.*, 2006). Verma and Sharma (2009) studied the prolongation of a gaseous plasma channel formed by a two-pulse technique for laser intensities below the tunnel ionization threshold. Kumar *et al.* (2011) developed a formalism for the formation of a parabolic radial density profile, $n(r) = (1 + n_2 r^2/r_0^2)$ by a sequence of two pulses and examined the focusing of a third intense pulse of spot size r_0 in the low laser intensity limit, where n_2 and r_2 are related to prepulses. Zhang *et al.* (2011) investigated the differential equation of the spot size of a Gaussian laser pulse in a preformed plasma channel including the effects of relativistic self-focusing, ponderomotive self-channeling, and preformed channel focusing. The existence of electromagnetic solitary waves should be helpful to enhance charged particle acceleration involving laser-plasma channel interaction.

Plasma channel, produced by radial expulsion of plasma electrons due to the large ponderomotive force of laser, introduces significant nonlocal effects on stimulated Raman scattering. Liu and Tripathi (1996) studied the stimulated Raman forward scattering (SRFS) of a non-relativistic laser pump in a performed cold plasma channel. Shvets and Li (2001) studied the Raman forward scattering in shallow plasma channels arising due to the radial shear of the plasma frequency and the existence of the weakly damped hybrid (electrostatic/electromagnetic) modes of the radially inhomogeneous plasma. The interplay of these two effects produces double-peaked spectra for the direct forward scattering in a channel. Panwar *et al.* (2012) investigated stimulated Raman forward scattering (SRFS) of an intense

Address correspondence and reprint requests to: Chang-Mo Ryu, Department of Physics, POSTECH, Hyoja-Dong San 31, KyungBuk, Pohang, South Korea, 790-784. E-mail: ryu201@postech.ac.kr

https://doi.org/10.1017/S0263034613000311 Published online by Cambridge University Press

short pulse laser in a plasma channel formed by two pre-laser pulses. Normalized growth rate of SRFS increase with density nonuniformity of plasma channels. However, in the presense of a deep plasma channel the focusing is ineffective to laser intensities, but growth rate increases with intensity of main laser pulse.

Linearly, polarized laser in a uniform plasma produces odd harmonics with power peaking at the third harmonic. The energy conversion efficiency is low as the wave number of the third harmonic k_3 does not match three times the wave number of the laser k_0 ($k_3 > 3k_0$), making it a nonresonant process. Introduction of a density ripple or a magnetic wiggler (Rax *et al.*, (1992; 1993; Liu *et al.*, 2008) of wave number $k_q = (k_3 - 3k_0)$ can turn the third harmonic generation into a resonant process, greatly enhancing the efficiency. Phase-matched relativistic harmonic generation in a plasma has observed experimentally for the first time by Chen *et al.* (2000). Third harmonic light is detected in forward direction by varying the temporal delay and the energy of the laser pulse. Shibu and Tripathi (1998) have studied the phase-matched third harmonic generation of a laser beam propagating through a plasma channel without non-uniformity and showed that the presence of a background density perturbation can account for phase-matching. Liu and Triapthi (2008) studied the resonant third harmonic generation of a Gaussian laser pulse in rippled density plasma created by a machining beam. The energy conversion efficiency scales as the square of plasma density and square of depth of density ripple. Kuo *et al.* (2007) have reported the enhancement of relativistic third harmonic generation by using an optically preformed periodic plasma waveguide. Resonant dependence of harmonic intensity on plasma density and density modulation parameters was also observed. Deepak *et al.* (2007) have carried out particel in cell (PIC) simulations of harmonic generation in a plasma density ripple and their scaling of efficiency with laser intensity, ripple amplitude, and plasma density. Sodha *et al.* (2009) investigated third harmonic generation caused by the self-focusing of a Gaussian electromagnetic beam in collisional plasmas. Self-focusing of the fundamental beam enhances the power of the third harmonic output indicating that the region of third harmonic generation is localized near the axis of the beam.

In the present work, we show that the effect of plasma channel non-uniformity on resonant third harmonic generation. A laser pulse can be successfully self-focused and compressed in underdense plasma due to relativistic mass nonlinearity and plasma channel non-uniformity. Here we consider a non-uniform plasma channel with a density ripple $n_q = n_{q0}e^{ik_q z}$, where $\vec{k}_q \| \vec{k}_0$. A linearly polarized main laser pulse $\vec{E}_0(\omega_0, \vec{k}_0)$ induces an oscillatory velocity $\vec{v}_0(\omega_0, \vec{k}_0)$ to the electrons and exerts a non-linear ponderomotive force $(\vec{v}_0 \times \vec{B}_0)$. Ponderomotive force producing oscillatory velocity $\vec{v}_{2\omega_0, 2k_0}$ and beats with n_q to produce a density oscillation $n_{2w_0,\ 2k_0+k_q}$. This density beats with $\vec{v}_0(\omega_0, \vec{k}_0)$ to produce a nonlinear current, resonantly driving the third harmonic when $(3k_0 + k_q)$ equals the third harmonic wave number.

We study the laser pulse self-focusing and compression through the non-uniform rippled plasma channel in Section 2. In Section 3, we analyze the resonant third harmonic generation including self-focusing and compression effects. The results are discussed in Section 4.

2. LASER PULSE COMPRESSION AND SELF-FOCUSING THROUGH A PRE-FORMED RIPPLED PLASMA CHANNEL

Consider a plasma channel with density ripple $n_q = n_{q0}e^{ik_q z}$ (Shibu & Tripathi, 1998), the equilibrium electron density becomes,

$$n(r, z) = (n_{e0} + n_{q0}e^{ik_q z})\left(1 + \frac{n_2}{n_{e0}}\frac{r^2}{r_2^2}\right), \tag{1}$$

where the electron density on channel axis $n_{e0} \gg n_{q0}$, plasma channel non-uniformity n_2/n_{e0}, and spot size r_2 are related to the properties of channel (Ashok *et al.*, 2011). The laser pulse propagates through rippled plasma channel with electric field,

$$\vec{E}_0 = \hat{x}A_0(r, z, t)e^{-i(\omega_0 t - k_0 z)}, \tag{2}$$

where $k_0 = (\omega_0/c)\eta_0$, η_0 is the refractive index of the plasma, and $A_0(r, z, t)$ is the slowly varying complex amplitude of the laser. At $z = 0$,

$$A_0|_{z=0}^2 = A_{00}^2 e^{-r^2/r_0^2}e^{-t^2/\tau_0^2}, \tag{3}$$

where r_0 and τ_0 are the beam radius (in cylindrical coordinates) and pulse width (in time), respectively. And A_{00} is the amplitude of the beam at axis. At $z > 0$, laser beam amplitude is modified as,

$$|A_0|^2 = \frac{A_{00}^2}{gf^2}e^{-r^2/r_0^2 f^2}e^{-t^2/\tau_0^2 g^2}, \tag{4}$$

where f and g represent the beam width parameter (in space) and pulse width parameter (in time), respectively. The electron response to laser pulse from momentum equation becomes,

$$m_e\gamma\frac{\partial\vec{v}_0}{\partial t} = -e\vec{E}_0, \tag{5}$$

where $-e$ and m_e are electronic charge and mass, respectively, and relativistic gamma factor $\gamma = (1 + (a_{00}^2 e^{-r^2/r_0^2 f^2}/e^{-t^2/\tau_0^2 g^2})/2gf^2)^{1/2}$ is described in terms of noramalized laser amplitude $a_{00}^2 = |e\,A_{00}/m_e\omega_0 c|^2$. Here we also have neglected $(\vec{v}_0 \times \vec{B}_0)$, because of its twice high frequency. The electron current density at

https://doi.org/10.1017/S0263034613000311 Published online by Cambridge University Press

the main laser frequency $\vec{J}_0 = -n(r)e\vec{v}_0$ gives,

$$\partial_t \vec{J}_0 = -n(r)e\partial_t \vec{v}_0 = n(r, z)\frac{e^2\vec{E}_0}{m_e\gamma}. \tag{6}$$

The wave equation governing the electric field of the pump laser beam in plasma can be drived from Maxwell's equations. Using Maxwell's equations in MKS units,

$$\nabla^2\vec{E}_0 - \nabla(\nabla\cdot\vec{E}_0) - \mu_0\frac{\partial\vec{J}_0}{\partial t} - \frac{1}{c^2}\frac{\partial^2\vec{E}_0}{\partial t^2} = 0 \tag{7}$$

where $c = 1/\sqrt{\mu_0\varepsilon_0}$ is the speed of light in free space. For a transverse electromagnetic fields (such as linear polarized) $\nabla\cdot\vec{E}_0 = 0$. Using Eq. (1) and Eq. (6) into wave equation Eq. (7).

$$2ik_0\frac{\partial}{\partial z'}A_0 + \nabla_\perp^2 A_0 + \beta\frac{\partial}{\partial\tau^2}A_0 - \left[k_0^2 - \frac{\omega_0^2}{c^2}\left(1 - \frac{\omega_{p0}^2/\gamma}{\omega_0^2}\left(1 + \frac{n_2}{n_{e0}}\frac{r^2}{r_2^2}\right)\right)\right]A_0 = 0, \tag{8}$$

where $\beta = \left(1/c^2\right)\sqrt{1 - \varepsilon_{eff0}/\varepsilon_{eff0}}$, and transforming the variables z and t to $z = z$ and $\tau = (t - z/\upsilon_g)$, respectively. Here the parallel variation of the amplitude A_0 in terms of z is assumed to be slower than the transverse one (in r), therefore terms in $\partial^2/\partial z'\partial\tau$ and $\partial^2/\partial z'^2$ can be neglected. The third term in Eq. (8) is known as the group velocity dispersion (GVD) term and it results in pulse compression when combined with (balanced by) nonlinearity. One can expand γ by using Taylor's expansion,

$$\frac{1}{\gamma}(r, t) = \frac{1}{\gamma_0}\left(1 + \frac{a_{00}^2 r^2/4r_0^2 gf^4}{1 + a_{00}^2/2gf^2} + \frac{a_{00}^2 t^2/4\tau_0^2 g^3 f^2}{1 + a_{00}^2/2gf^2}\right), \tag{9}$$

where $\gamma_0 = (1 + a_{00}^2/2)^{1/2}$ is the value of γ on the axis. We get the total dielectric constatnt,

$$\varepsilon(r, z, t) = \varepsilon_{eff0} + \varepsilon_{2r}r^2 + \varepsilon_{2t}t^2, \tag{10}$$

where

$$\varepsilon_{2r} = \frac{-\omega_p^2}{\omega_0^2 r_0^2\gamma_0}\Phi_{2r},\ \Phi_{2r} = \left(\frac{n_2}{n_{e0}}\frac{r_0^2}{r_2^2} + \frac{a_{00}^2}{4gf^4\left(1 + a_{00}^2/2gf^2\right)}\right),$$
$$\varepsilon_{2t} = -\frac{\omega_p^2}{\omega_0^2\tau_0^2\gamma_0}\Phi_{2t},\quad \Phi_{2t} = \frac{a_0^2}{4g^3f^2\left(1 + a_{00}^2/2gf^2\right)}. \tag{11}$$

and

And using $k_0 = \left(\omega_0/c\right)\sqrt{\varepsilon_{eff0}}$, we get the wave equation Eq. (9),

$$\left(2ik_0\frac{\partial}{\partial z'} + \nabla_\perp^2 + \beta\frac{\partial^2}{\partial\tau^2}\right)A_0 + \frac{\omega_0^2}{c^2}\left(\varepsilon_{2r}r^2 + \varepsilon_{2t}t^2\right)A_0 = 0. \tag{12}$$

This equation describes the propagation of laser pulse through the plasma with relativistic mass nonlinearity and plasma channel non-uniformity. In the simplified analytical model, we take into account the nonlinearity by relativistic mass and plasma channel non-uniformity, and neglect electron density perturbation. Eq, (12) is a nonlinear Schrödinger equation, where third term in the first bracket representing the dispersion broadening and second bracket term representing the nonlinear compression. When the two effects balance each other, one obtains a coherent structure in the form of a solitary wave. Now, following Akhmanov *et al.* (1996) and Sodha *et al.* (1974) to evaluate the pulse evolution we introduce an eikonal approximation, $A_0 = A_{00}\exp(iS)$, where $A_{00}(r, z', \tau)$ and $S(r, z', \tau)$ are real functions and separate out the real and imaginary parts of the resulting equations,

$$-2k_0\left(\frac{\partial S}{\partial z'}A_{00}\right) + \left[\frac{1}{r}\left(\frac{\partial A_{00}}{\partial r}\right) + \frac{\partial^2 A_{00}}{\partial r^2} - A_{00}\left(\frac{\partial S}{\partial r}\right)^2\right] + \beta\left[\frac{\partial^2 A_{00}}{\partial\tau^2} - A_{00}\left(\frac{\partial S}{\partial\tau}\right)^2\right] + \frac{\omega_0^2}{c^2}\left(\varepsilon_{2r}r^2 + \varepsilon_{2\tau}\tau^2\right)A_{00} = 0, \tag{13}$$

and

$$k_0\frac{\partial A_{00}^2}{\partial z'} + \left(\frac{\partial^2 S}{\partial r^2} + \frac{1}{r}\frac{\partial S}{\partial r}\right)A_{00}^2 + \frac{\partial A_{00}^2}{\partial r}\frac{\partial S}{\partial r} + \beta\left[\frac{\partial A_{00}^2}{\partial\tau}\frac{\partial S}{\partial\tau} + A_{00}^2\frac{\partial^2 S}{\partial r^2}\right] = 0. \tag{14}$$

The coupled set of equations for A_{00}^2 and S are solved in the paraxial approximation by expanding S only to the first power of r^2 and r^2 such as,

$$S(r, z', \tau) = S_0(z') + S_{2r}(z')\frac{r^2}{r_0^2} + S_{2r}(z')\frac{\tau^2}{\tau_0^2}, \tag{15}$$

where function $f(z')$ and $g(z')$ are,

$$S_{2r}(z') = \frac{1}{2f}\frac{\partial f}{\partial z'} \quad \text{and} \quad S_{2r}(z') = \frac{1}{2g}\frac{\partial f}{\partial z'}, \tag{16}$$

and $S_0(z')$ is the axial phase. We obtain the beam width and pulse width parameter equations by collecting coefficient of r^2 and r^2 in terms of dimensionless distance $\xi = z/R_d$,

$$\frac{\partial^2 f}{\partial\xi^2} = \frac{1}{f^3} - \frac{\omega_{p0}^2\Phi_{2r}}{\gamma_0\omega_0^2}\frac{R_d^2}{r_0^2}f, \tag{17}$$

and

$$\frac{\partial^2 g}{\partial\xi^2} = \frac{\beta^2}{g^3}\frac{r_0^4}{r_0^4} - \beta\frac{\omega_{p0}^2\Phi_{2t}}{\gamma_0\omega_0^2}\frac{R_d^2}{r_0^2}g, \tag{18}$$

where $R_d = k_0 r_0^2$ is the diffraction length, the first and second

https://doi.org/10.1017/S0263034613000311 Published online by Cambridge University Press

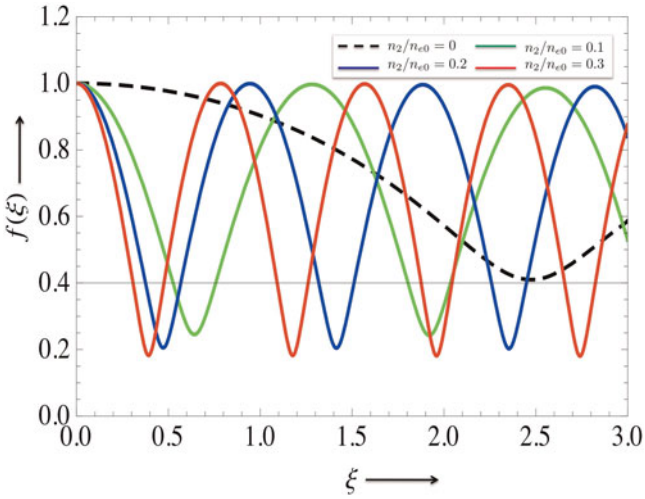


Fig. 1. (Color online) Variation of beam width parameter f with respect to the normalized propagation distance $\xi = z'/R_d$ for a normalized laser amplitude $a_{00} = 0.3$ through different plasma channels with non-uniformities $n_2/n_{e0} = 0$, 0.1, 0.2 and 0.3. The other parameters are $\omega_0 = 2.8195 \times 10^{14}$ s.$^{-1}$, $r_0 = 14$ μm, $n_{e0} = 0.85 \times 10^{24}$ m^{-3}, $\tau_0 = 10$ ps and $r_2 = 16$ μm.

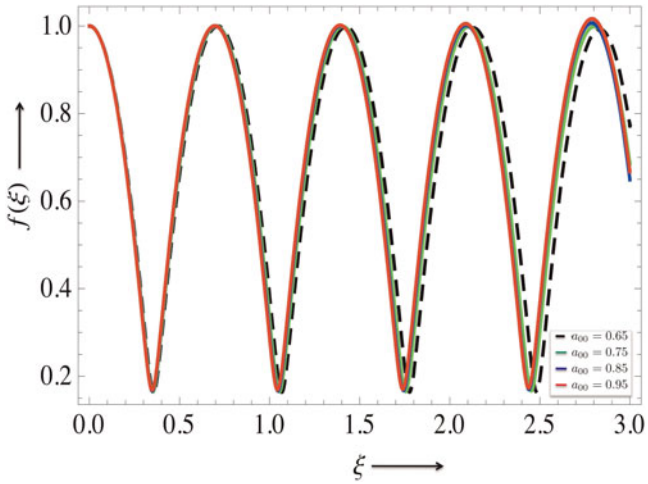


Fig. 3. (Color online) Variation of beam width parameter f with the normalized propagation distance $\xi = z/R_d$ for different laser amplitudes $a_{00} = 0.65$, 0.75, 0.85, and 0.95 through a deep plasmas channel with non-uniformity $n_2/n_{e0} = 0.3$. The other parameters are $\omega_0 = 2.8195 \times 10^{14}$ s.$^{-1}$, $r_0 = 14$ μm, $n_{e0} = 0.85 \times 10^{24}$ m^{-3}, $\tau_0 = 10$ps and $r_2 = 16$ μm.

term in the right-hand side of above Eq. (17) contribute to the the diffraction divergence and nonlinear self-focusing, respectively. Coupled equations contain nonlinear corrections by relativistic mass and plasma channel non-uniformity. So the self-focusing and compression of main pulse can be controlled by the plasma channel non-uniformity and laser intensity. The boundary conditions at $\xi = z' = 0$ for an initially plane wavefront are $f = g = 1$, $\partial f/\partial \xi = \partial g/\partial \xi = 0$ and $S_0 = 0$. In Figures 1 and 2, we plotted the variation of f and g with respect to ξ for main laser pulse frequency $\omega_0 = 2.8195 \times 10^{14}/\text{s.}^{-1}$, spot size $r_0 = 14$ μm, $\tau_0 = 10$ ps and normalized pump amplitude $a_{00} = e\ |E00|/m_e\omega_0 c = 0.3$. The other parameters are $n_{e0} = 0.85 \times 10^{24}$ m^{-3}, $\omega_{p0}/\omega_0 = 0.18$, and the spot size of second laser beam, $r_2(>r_0) = 16$ μm. The main laser pulse shows the periodic focusing (Fig. 1) and compression (Fig. 2) inside the plasma channels, it increases with increasing density non-uniformity of the plasma channels with $n_2/n_{e0} = 0.1$, 0.2, and 0.3. For the main laser pulse with different intensities, $a_{00} = 0.65$, 0.75, 0.85, and 0.95 through a deep plasma channel with non-uniformity $n_2/n_{e0} = 0.3$, the variation of f and g with respect to ξ is plotted in Figures 3 and 4, and other plasma paremeters are the same as (Fig. 1). The Self-focusing behavior for different intensities show a similarity due to the ineffectiveness of intensity dependent nonlinearity (Fig. 3), however, pulse compression increases with the main laser intensity (Fig. 4).

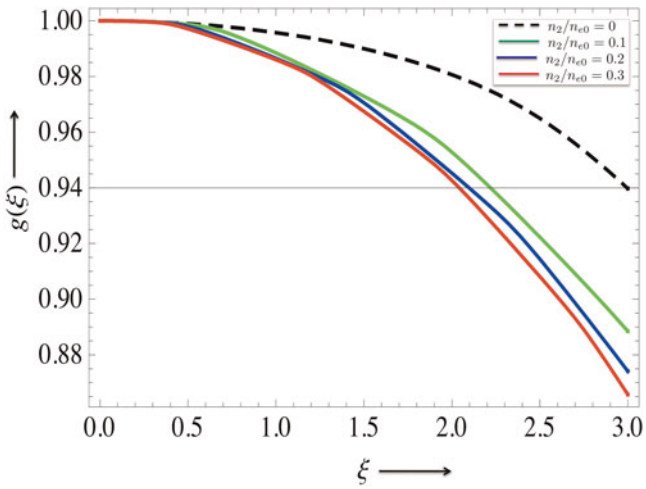


Fig. 2. (Color online) Variation of temporal parameter g with the normalized propagation distance $\xi = z/R_d$ for a normalized laser amplitude $a_{00} = 0.3$ in different plasma channels for the parameters same as in Figure 1.

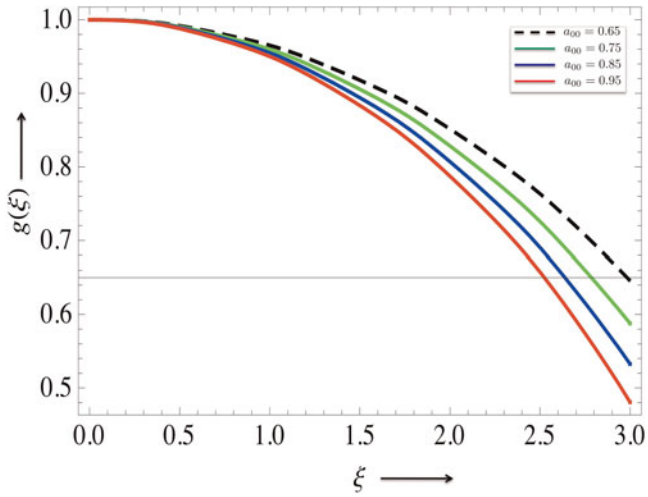


Fig. 4. (Color online) Variation of temporal parameter g with the normalized propagation distance $\xi = z/R_d$ for different laser amplitudes $a_{00} = 0.65$, 0.75, 0.85, and 0.95through a deep plasma channel with non-uniformity $n_2/n_{e0} = 0.3$ for the same parameters same as in Figure 3.

https://doi.org/10.1017/S0263034613000311 Published online by Cambridge University Press

3. THIRD HARMONIC GENERATION

Laser pulse exerts a pondermotive force on electrons at second harmonic ($2\omega_0$, $2k_0$),

$$\vec{F}_{2\omega_0,2k_0} = -\frac{e}{2}\left(\vec{v}_0 \times \vec{\beta}_0\right) = \frac{e^2}{2m_e i\omega_0 c}\hat{z}\eta_0 A_0^2(r, z, t)e^{-2i\Psi}, \quad (19)$$

where $\Psi = (\omega_0 t - k_0 z)$. Ponderomotive force $\vec{F}_{2\omega_0,2k_0}$ is primarily along $\hat{z}$ direction and its electron response will be only in the z-direction. The electron oscillatory velocity due to ponderomotive force becomes,

$$\vec{v}^{NL}_{2\omega_0} = \frac{a_{00}^2 c}{4\gamma}\hat{z}\eta_0 e^{-2i\Psi}. \quad (20)$$

This oscillatory velocity couples with ripple density n_q, through the equation of continuity to produce a density perturbation at (2ω, $2k_0 + k_q$),

$$n_{2\omega_0,2k_0+k_q} = \frac{1}{2}n(r)(2\vec{k}_0 + k_q)\cdot\frac{\vec{v}_{2\omega_0,2k_0}}{2\omega_0} \quad (21)$$

$$\approx -n_{q0}\left(1 + \frac{n_2}{n_{e0}}\frac{r^2}{r_2^2}\right)\frac{a_{00}^2}{8\gamma}\eta_0 e^{-i[2\omega_0 t-(2k_0+k_q)z]}. \quad (22)$$

The perturbation Eq. (22) beats with electron velocity Eq. (5) to give the third harmonic nonlinear current density at ($3\omega_0$, $3k_0 + k_q$),

$$\vec{J}^{NL}_{3\omega_0,3k_0+k_q} = -\frac{e}{2}n_{2\omega_0,2k_0+k_q}\vec{v}_{\omega_0,k_0}$$
$$= -\hat{x}\frac{i}{16\gamma^2}n_{q0}eca_{00}^3\eta_0 e^{-i(3\omega_0 t-(3k_0+k_q)z)}. \quad (23)$$

The linear current density due to the self-consistent second harmonic field, $\vec{E}_{3\omega_0}$ is

$$\vec{J}^{L}_{3\omega_0} = -\frac{n(r)e^2\vec{E}_{3\omega_0}}{3im_e\omega_0} \approx -n_{e0}\left(1 + \frac{n_2}{n_{e0}}\frac{r^2}{r_2^2}\right)\frac{e^2\vec{E}_{3\omega_0}}{3im_e\omega_0}, \quad (24)$$

and the wave equation for third harmonic field,

$$\nabla^2\vec{E}_{3\omega_0} - \nabla\left(\nabla\cdot\vec{E}_{3\omega_0}\right) - \mu_0\frac{\partial\vec{J}^{L}_{3\omega_0}}{\partial t} - \frac{1}{c^2}\frac{\partial^2\vec{E}_{3\omega_0}}{\partial t^2} = \mu_0\frac{\partial\vec{J}^{NL}_{3\omega_0}}{\partial t}. \quad (25)$$

Using Eq. (22) and Eq. (24) into Eq. (22) wave equation becomes,

$$\nabla^2\vec{E}_{3\omega_0} + \frac{\omega_{p0}^2}{c^2}\left(1 + \frac{n_2}{n_{e0}}\frac{r^2}{r_2^2}\right)\vec{E}_{3\omega_0} - \frac{1}{c^2}\frac{\partial^2\vec{E}_{3\omega_0}}{\partial t^2}$$
$$= \hat{x}S_3 e^{-i(3\omega_0 t-(3k_0+k_q)z)}, \quad (26)$$

where $S_3 = -3n_{q0}e\omega_0 a_{00}^3\eta_0/16\varepsilon_0 c\gamma^2$. We may write $\vec{E}_{3\omega_0} = \hat{x}A_{3\omega_0}(r, z, t)e^{-(3\omega_0 t-k_3 z)}$ and in terms of slowly varying laser amplitude by using the WKB approximation. Transforming the variables z and t to z and $t' = (t - z/v_{g3\omega_0})$, respectively, and using third harmonic group velocity, $v_{g3\omega_0} = k_3c^2/3\omega_0$,

$$2ik_3\frac{\partial A_{3\omega_0}}{\partial z'} + \nabla_\perp^2 A_{3\omega_0} + \left(\frac{9\omega_0^2 - \omega_{p0}^2/\gamma_0}{c^2} - k_3^2\right)A_{3\omega_0}$$
$$-\frac{\omega_{p0}^2}{c^2}\frac{n_2}{n_{e0}}\frac{r^2}{r_2^2}A_{3\omega_0} = S_3 e^{-i\Delta z'}, \quad (27)$$

where $\Delta = (k_3 - 3k_0 - k_q)$. We can also write the above equation as,

$$2ik_3 r_3^2\frac{\partial A_{3\omega_0}}{\partial z'} + \frac{\partial^2 A_{3\omega_0}}{\partial\rho_3^2} + \frac{1}{\rho_3}\frac{\partial A_{3\omega_0}}{\partial\rho_3} + (\lambda_3 - \rho_3^2)A_{3\omega_0} = S_3 r_3^2 e^{-i\Delta z'}, \quad (28)$$

where $r_3^2 = ((c^2 r_2^2 n_{e0})/n_2\omega_{p0}^2)^{1/2}$ and $\rho_3 = r/r_3$. To solve the above equation, we express $A_{3\omega_0}$ as,

$$A_{3\omega_0} = A_{3\omega_0}(z')\Psi_n(\rho_3), \quad (29)$$

where $\Psi_n(\rho_3)$ are the eigen-functions satisfying,

$$\frac{\partial^2\Psi_n}{\partial\rho_3^2} + \frac{1}{\rho_3}\frac{\partial\Psi_n}{\partial\rho_3} + (\lambda_3 - \rho_3^2)\Psi_n = 0, \quad (30)$$

with $\lambda_3 = (2n + 1)$. This equation gives an eigen function, $A_{3\omega_0} = \rho_3^n e^{-\rho_3^2/2}$. For $n = 0$ mode, the eigen function $\Psi_n(\rho_3) = e^{-\rho_3^2/2}$ is Gaussian and eigen value $\lambda_3 = 1$,

$$k_3^2 = \frac{1}{c^2}\left(9\omega_0^2 - \frac{\omega_{p0}^2}{\gamma_0} - \frac{c^2}{r_3^2}\right). \quad (31)$$

Now substituting the above solution to the third harmonic wave equation and multiplying the resulting equation by Ψ^* and integrating from $-\infty$ to ∞ one obtains,

$$\frac{\partial A_{3\omega_0}}{\partial z'} = \frac{S_3}{2ik_3}e^{-i\Delta z'}. \quad (32)$$

For a Gaussian pulse $A_0^2 = (A_{00}^2/2g\,f^2)e^{-r^2/r_0^2 f^2}\,e^{-\tau^2/\tau_0^2 g^2}$ and $\gamma = [1 + (a_{00}^2/2g\,f^2)e^{-r^2/r_0^2 f^2}\,e^{-\tau^2/\tau_0^2 g^2}]^{1/2}$ are functions of r and t. For a given k_q, one cannot have phase matching ($\Delta = 0$) for third harmonic generation all r and t (Liu & Tripathi, 2008). If one matches the ripple wave number at the peak of the laser pulse at '$r = 0$' and '$t = 0$' i.e.,

$$k_q = (k_3 - 3k_0) = \frac{4}{3}\frac{\omega_{p0}^2}{\omega_0^2\gamma_0}\frac{\omega_0}{c}, \quad (33)$$

https://doi.org/10.1017/S0263034613000311 Published online by Cambridge University Press

where $\gamma_0 = (1 + a_{00}^2/2)^{1/2}$, then at other r and t,

$$\Delta = k_q\left(\frac{\gamma_0}{\gamma(r,t)}\frac{\omega_p^2(r,t)}{\omega_{p0}^2} - 1\right). \tag{34}$$

Using Eq. (34) into Eq. (32) and after integrating with perfect to z', we get a third harmonic amplitude,

$$|a_{3\omega_0}|^2 = \left(\frac{1}{32}\frac{n_{q0}}{n_{e0}}\frac{\omega_0}{k_3 c}\frac{\omega_{p0}^2}{\omega_0^2}\frac{a_{00}^3}{\gamma^2}\right)^2 k_0^2 \times \frac{Sin^2\left[\frac{k_q}{2}\left(\frac{r_0}{r(r,t)}\frac{\omega_p^2(r,t)}{\omega_{p0}^2} - 1\right)z'\right]}{\left[\frac{k_q}{2}\left(\frac{r_0}{r(r,t)}\frac{\omega_p^2(r,t)}{\omega_{p0}^2} - 1\right)\right]^2}, \tag{35}$$

where the third harmonic normalized amplitude is normalized as, $|a_{3\omega_0}|^2 = |eA_{3\omega_0}/3m_e\omega_0 c|^2$. For

$$z' < \frac{2}{k_q\left(\frac{\gamma_0}{\gamma(r,t)}\frac{\omega_p^2(r,t)}{\omega_{p0}^2} - 1\right)}, \tag{36}$$

we get the normalized third harmonic amplitude,

$$|a_{3\omega_0}|^2 \approx \left(\frac{1}{32}\frac{n_{q0}}{n_{e0}}\frac{\omega_0}{k_3 c}\frac{\omega_{p0}^2}{\omega_0^2}k_0 z'\right)^2\frac{a_{00}^6}{\gamma^4}. \tag{37}$$

The total power $P_{3\omega_0}$ of the third harmonic across the transverse cross section at any value of z' can be obtained by integrating $a_{3\omega_0}\, a_{3\omega_0}{}^*$ over r from '0' to ∞ (Sodha *et al.*, 2009) and t from $-\infty$ to ∞ (Liu & Tripathi, 2008) i.e.,

$$P_{3\omega_0} = \frac{c\eta_{3\omega_0}\varepsilon_0}{2}\int_0^\infty \int_{-\infty}^{\infty} a_{3\omega_0} a_{3\omega_0}^* \, 2\pi r dr dt, \tag{38}$$

and initialy pump power at $z = 0$ and $t = 0$, $P_{\omega_0} = (\eta_{\omega_0}/2)\pi r_0^2 a_{00}^2$. So we get the conversion efficiency of third harmonic across the transverse cross section,

$$\frac{P_{3\omega_0}}{P_{\omega_0}} = \left(\frac{1}{96}\frac{n_{q0}}{n_{e0}}\frac{\omega_{p0}^2}{\omega_0^2}k_0 R_d\right)^2 a_{00}^4\xi^2 \times \left(\frac{1}{\gamma_0^4} + \frac{a_{00}^2/4gf^4}{\gamma_0\left(1 + a_{00}^2/2gf^2\right)^{5/2}} + \frac{a_{00}^2/8g^5f^2}{\gamma_0\left(1 + a_{00}^2/2gf^2\right)^{5/2}}\right). \tag{39}$$

One can straight forwardly obtain from the dependence of the third harmonic power on beam width parameter f, pulse width parameter g and intensity of the fundamental laser beam, and other plasma parameters.

We numerically plotted the energy conversion ratio $P_{3\omega_0}/P_{1\omega_0}$ with respect to the normalized propagation distance $\xi = z'/R_d$ in different plasma channels in Figure 5. The presence of plasma channel nor-uniformity guide the main laser pulse and increase the self-focusing in Figure 1 and compression Figure 2, which further increase the energy conversion ratio $P_{3\omega_0}/P_{1\omega_0}$ with distances of propagation. In Figure 6, the presense of a nonuniform deep plasma channel $n_2/n_{e0} = 0.3$ focusing is independent of the laser intensity. However, the pulse compression and the energy conversion ratio increase with the intensity of the main laser pulse.

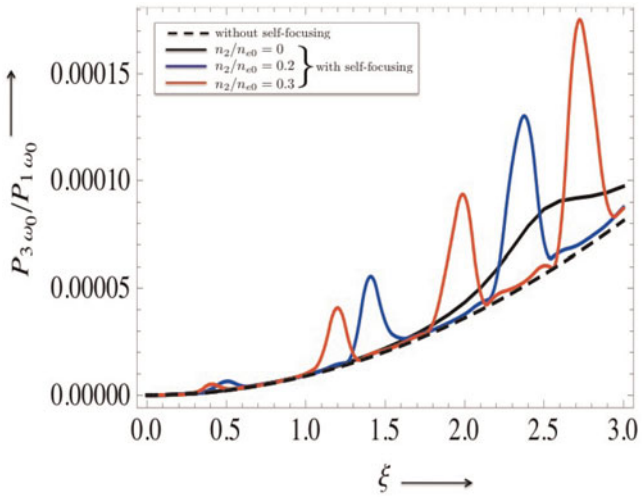


Fig. 5. (Color online) Variation of energy conversion ratio '$\eta = P_{3\omega_0}/P_{1\omega_0}$' with respect to the normalized propagation distance '$\xi = z'/R_d$' for a normalized laser amplitude $a_{00} = 0.3$ through different plasma channels with non-uniformities $n_2/n_{e0} = 0$, 0.2 and 0.3. The other parameters are $\omega_0 = 2.8195 \times 10^{14}\text{Sec}^{-1}$, $r_0 = 14\mu m$, $n_{e0} = 0.85 \times 10^{24}\,\text{m}^{-3}$, $\tau_0 = 10\text{ps}$ and $r_2 = 16\mu m$.

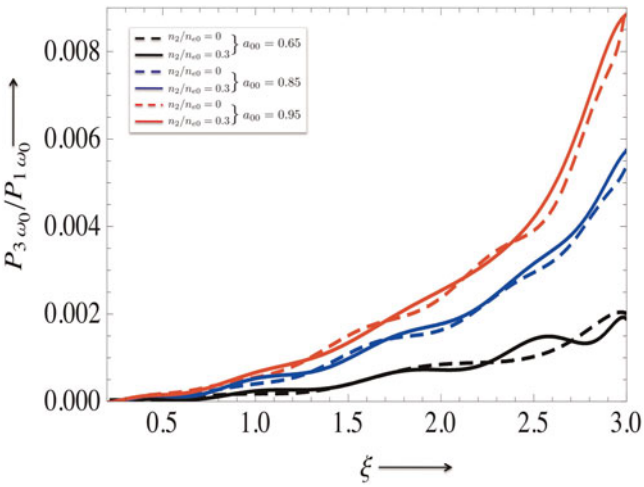


Fig. 6. (Color online) Variation of energy conversion ratio '$P_{3\omega_0}/P_{1\omega_0}$' with respect to the normalized propagation distance '$\xi = z'/R_d$' for different laser amplitudes $a_{00} = 0.65$, 0.85 and 0.95 through a deep plasma channels with non-uniformity $n_2/n_{e0} = 0.3$. The other parameters are $\omega_0 = 2.8195 \times 10^{14}\text{Sec}^{-1}$, $r_0 = 14\mu m$, $n_{e0} = 0.85 \times 10^{24}\,\text{m}^{-3}$, $\tau_0 = 10\text{ps}$ and $r_2 = 16\mu m$.

4. CONCLUSIONS

We have carried out an analysis to understand the effect of plasma channel non-uniformity on resonant third harmonic

https://doi.org/10.1017/S0263034613000311 Published online by Cambridge University Press

generation due to self-focusing effect. Two pre-laser pulses produce an axially non-uniform rippled plasma channel. After ns, main pulse of intensity $a_{00} = 0.30$ shows a periodic focusing and compression in non-uniform plasma channels. Self-focusing and pulse compression increase with the increase in non-uniformity of the plasma channel with $n_2/n_{e0} = 0.1$, 0.2, and 0.3 in Fig. 1 and Fig. 2 respectively. Self-focusing is independent of main laser intensities in a deep plasma channel with nouniformity $n_2/ne = 0$ in Figure 3, however pulse compression increases due to laser intensity Figure 4. The effect of the density ripple of wave number $k_q = 4\omega_p^2/3m_e\omega_0 c\gamma_0$, makes the laser third harmonic generation a resonant process. Since the beam width parameter keeps on changing in a periodic manner and pulse width parameter decreases with the dimensionless distance of propagation ξ, the power of the third harmonic also shows a periodic behavior. As the beam width parameter attains a minimum value, the irradiance of the fundamental beam and consequently the power of the third harmonic power gets enhanced. In Figure 5, in the presence of plasma channel, the third harmonic power increases with non-uniformity $n_2/n_{e0} = 0.1$, 0.2, and 0.3. In the presence of deep cavitation $n_2/n_{e0} = 0.3$, the third harmonic power has less self-focusing periodic character and increases with the intensity of the main laser pulse in Figure 6.

ACKNOWLEDGMENTS

The work is supported by R&D Program through the National Fusion Research Institute of Korea (NFRI) and the grants NRF-2011-0026107 from the National Research Foundation of Korea.

REFERENCES

Akhmanov, S.A., Sukhorukov, A.P. & Khokhlov, R. (1966). *Sov. Phys. JETP* **23**, 1025.

Chen, S.-Y., Maksimchuk, A., Esarey, E. & Um- stadter, D. (2000). Observation of phase-matched relativistic harmonic generation. *Phys. Rev. Lett.* **84**, 5528–5531.

Dahiya, D., Sajal, V. & Sharma, A.K. (2007). Phase- matched second- and third-harmonic generation in plasmas with density ripple. *Phys. Plasmas* **14**, 123104.

Durfee, C.G., Lynch, J. & Milchberg, H.M. (1995). Development of a plasma waveguide for high-intensity laser pulses. *Phys. Rev. E* **51**, 2368–2389.

Durfee, C.G. & Milchberg, H.M. (1993). Light pipe for high intensity laser pulses. *Phys. Rev. Lett.* **71**, 2409–2412.

Ehrlich, Y., Cohen, C., Zigler, A., Krall, J., Sprangle, P. & Esarey, E. (1996). Guiding of high intensity laser pulses in straight and curved plasma channel experiments. *Phys. Rev. Lett.* **77**, 4186–4189.

Esarey, E., Schroeder, C.B. & Leemans, W.P. (2009). Physics of laser-driven plasma-based electron accelerators. *Rev. Mod. Phys.* **81**, 1229–1285.

Esarey, E., Sprangle, P., Krall, J. & Ting, A. (1997). Self-focusing and guiding of short laser pulses in ionizing gases and plasmas. *IEEE J. Quan. Electron.* **33**, 1879–1914.

Geddes, C.G.R., Toth, C., van Tilborg, J., Esarey, E., Schroeder, C.B., Bruhwiler, D., Nieter, C., Cary, J. & Leemans, W.P. (2004). High-quality electron beams from a laser wakefield accelerator using plasma-channel guiding. *Nat.* **431**, 538–541.

Geddes, C.G.R., Toth, C., van Tilborg, J., Esarey, E., Schroeder, C.B., Cary, J. & Lee- mans, W.P. (2005). Guiding of relativistic laser pulses by preformed plasma channels. *Phys. Rev. Lett.* **95**, 145002.

Korobkin, D.V., Nam, C.H., Suckewer, S. & Goltsov, A. (1996). Demonstration of soft X-ray lasing to ground state in Li^3. *Phys. Rev. Lett.* **77**, 5206–5209.

Kumar, A., Dahiya, D. & Sharma, A.K. (2011). Laser prepulse induced plasma channel formation in air and relativistic self focusing of an intense short pulse. *Phys. Plasmas* **18**, 023102.

Kuo, C.-C., Pai, C.-H., Lin, M.-W., Lee, K.-H., Lin, J.-Y., Wang, J. & Chen, S.-Y. (2007). Enhancement of relativistic harmonic generation by an optically preformed periodic plasma waveguide. *Phys. Rev. Lett.* **98**, 033901.

Leemans, W.P., Nieter, B., Gonsalves, A.J., Tth, C., Nakamura, K., Geddes, C.G.R., Esarey, E., Schroeder, C.B. & Hooker, S.M. (2006). GeV electron beams from a centimetre-scale accelerator. *Nat. Phys.* **2**, 696–699.

Liu, C.S. & Tripathi, V.K. (1996). Stimulated Raman scattering in a plasma channel. *Phys. Plasmas* **3**, 3410.

Liu, C.S. & Tripathi, V.K. (2008). Third harmonic generation of a short pulse laser in a plasma density ripple created by a machining beam. *Phys. Plasmas* **15**, 023106.

Milchberg, H.M., Durfee III, C.G. & McIlrath, T.J. (1995). High-order frequency conversion in the plasma waveguide. *Phys. Rev. Lett.* **75**, 2494–2497.

Nikitin, S.P., Antonsen, T.M., Clark, T.R., Yuelin, L. & Milchberg, H.M. (1997). Guing of intense femtosecond pulses in preformed plasma channels. *Opt. Lett.* **22**, 1787–1789.

Panwar, A., Kumar, A. & Ryu, C.M. (2012). Stimulated Raman forward scattering of laser in a pre-formed plasma channel. *Laser Part. Beams* **18**, 023102.

Rax, J.M. & Fisch, N.J. (1992). Third-harmonic generation with ultrahigh-intensity laser pulses. *Phys. Rev. Lett.* **69**, 772–775.

Rax, J.M. & Fisch, N.J. (1993). Phase-matched third harmonic generation in a plasma. *IEEE Trans. Plasma Sci.* **21**, 105.

Shibu, S. & Tripathi, V.K. (1998). Phase matched resonant third harmonic generation of laser radiation in a plasma channel: non local effects. *Phys. Lett. A* **99**, 99–102.

Shvets, G. & Li, X. (2001). Raman forward scattering in plasma channels. *Phys. Plasmas* **8**, 8.

Sodha, M.S., Faisal, M. & Verma, M.P. (2009). Effect of self-focusing on third harmonic generation by a Gaussian beam in a collisional plasma. *Phys. Plasmas* **16**, 082340.

Sodha, M.S., Ghatak, A.K. & Tripathi, V.K. (1974). *Self Focusing of Laser Beams in Dielectrics, Plasmas and Semiconductors*. Delhi: Tata McGraw-Hill.

Spence, D.J., Butler, A. & Hooker, S.M. (2001). First demonstration of guiding of high-intensity laser pulses in a hydrogen-filled capillary discharge waveguide. *J. Phys. B: At. Mol. Opt* **34**, 4103.

Verma, U. & Sharma, A.K. (2009). Effect of self focusing on the prolongation of laser produced plasma channel. *Laser Part. Beams* **27**, 33–39.

Zhang, S., Xie, B.-S., Hong, X.-R., Wu, H.-C. & Zhao, X.-Y. (2011). Solitary waves of laser pulse in a plasma channel. *Phys. Plasmas* **18**, 033104.

https://doi.org/10.1017/S0263034613000311 Published online by Cambridge University Press